

## Stability of a Helmholtz Velocity Profile in a Continuously Stratified, Infinite Boussinesq Fluid—Applications to Clear Air Turbulence

RICHARD S. LINDZEN

*Center for Earth and Planetary Physics, Harvard University, Cambridge, Mass. 02138*

(Manuscript received 27 March 1974)

### ABSTRACT

The Kelvin-Helmholtz problem deals with the stability of fluids where both shear and stable stratification are restricted to a layer. In observed shear instability in the atmosphere, stable stratification rarely disappears outside the shear zone. In order to get some idea of the implications of this fact, I have investigated the stability properties of a particularly simple configuration: a Helmholtz velocity profile in a continuously stratified, infinite Boussinesq fluid. For a basic discontinuity  $2U$  and Brunt-Väisälä frequency  $N$ , I find that perturbations with horizontal wavenumbers  $k$ , such that  $k^2 > N^2/(2U^2)$ , are unstable and decay away from the shear zone. In addition, the shear zone is capable of supplying energy to neutral internal gravity waves, for which  $k^2 < N^2/U^2$ , which propagate away from the shear zone. A particular wavenumber,  $k^2 = N^2/(2U^2)$ , is shown to be most efficient at carrying energy away from the shear zone. However, additional calculations suggest that for the configuration considered, instabilities ought to be more effective than waves in smoothing the original shear. Comparison with observations suggests, on the other hand, that the waves dominate observed disturbances. The reasons for this are discussed. It is suggested that the waves are enhanced by reflections from the earth's surface which were ignored in the calculations.

### 1. Introduction

While the existence of clear air turbulence is usually attributed to the Kelvin-Helmholtz instability of shear zones generally associated with the jet stream, it is also frequently noted that there exist layered structures in the neighborhood of the shear zones (Ottersten *et al.*, 1973) which are more reminiscent of internal gravity waves than of Kelvin-Helmholtz instabilities where the unstable perturbation tends to decay away from the unstable interface [see Drazin and Howard (1966) for a review of Kelvin-Helmholtz instability]. Now, in the usual Kelvin-Helmholtz problem, both stratification and shear are confined to a layer; hence the wherewithal for internal gravity waves away from this layer is absent [see Hines (1960) for a review of internal gravity waves]. This situation would be altered if the fluid were everywhere stably stratified. It is the purpose of this paper to examine the simplest problem involving shear flow in a continuously stratified fluid, namely, the stability of a Helmholtz velocity profile in an infinite Boussinesq fluid with constant stratification. I will show that stratification inhibits instability for small values of horizontal wavenumber; however, at small wavenumbers I will show that there exist neutral (not growing in time) solutions in the form of internal gravity waves which propagate energy away from the shear layer. The coexistence of internal gravity waves and instabilities appears consistent with observed cases of clear air turbulence. Moreover, both the neutral internal gravity waves (by virtue of their ability to propagate energy and momentum), and the instabilities (by virtue of their growth) contribute to the smoothing of the shear zone. However, by means of some crude

estimates, I will show that the instabilities are *a priori* likely to be of primary importance in dissipating the shear zone. In Section 7, it will be seen that observations do not, however, support this conclusion. Possible reasons for this are discussed in Section 8.

### 2. Model and equations

Our basic state consists in a Boussinesq fluid with a constant Brunt-Väisälä frequency  $N$ , given by

$$N^2 = -\frac{g}{\rho_0} \frac{d\rho_0}{dz}, \tag{1}$$

where  $\rho_0$  is the basic density distribution,  $g$  gravitational acceleration, and  $z$  height;  $\rho_0$  is taken to be constant unless differentiated. The basic velocity profile  $U_0 = +U$  for  $z > 0$  and  $U_0 = -U$  for  $z < 0$  is shown in Fig. 1. I now investigate the behavior of small two-dimensional ( $x$  and  $z$  directions) perturbations on this basic state. The equations for such perturbations are

$$\frac{\partial u'}{\partial t} + U_0 \frac{\partial u'}{\partial x} = -\frac{1}{\rho_0} \frac{\partial p'}{\partial x}, \tag{2}$$

$$\frac{\partial w'}{\partial t} + U_0 \frac{\partial w'}{\partial x} = -\frac{1}{\rho_0} \frac{\partial p'}{\partial z} - g \frac{\rho'}{\rho_0}, \tag{3}$$

$$\frac{\partial \rho'}{\partial t} + U_0 \frac{\partial \rho'}{\partial x} + w' \frac{d\rho_0}{dz} = 0, \tag{4}$$

$$\frac{\partial u'}{\partial x} + \frac{\partial w'}{\partial z} = 0, \tag{5}$$

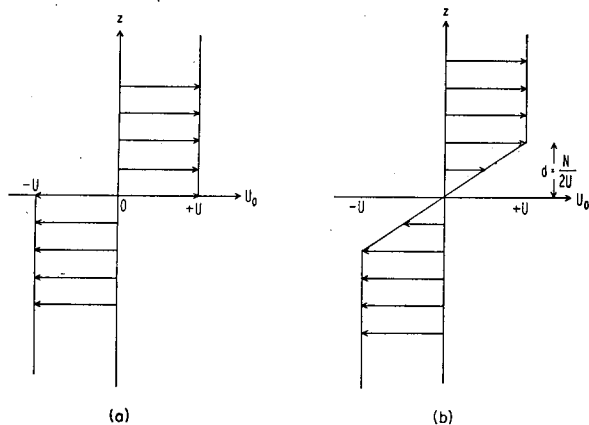


FIG. 1. Helmholtz velocity profiles, without smoothing (a) and smoothed so that  $Ri = \frac{1}{2}$  (b).

where  $u'$  and  $w'$  are the horizontal and vertical velocity perturbations, respectively,  $p'$  the pressure perturbation and  $\rho'$  the density perturbation. Seeking solutions of the form

$$f' = f(z)e^{ik(x-ct)}, \quad (6)$$

one obtains the following equation for  $w$ :

$$\frac{d^2w}{dz^2} + \left[ \frac{N^2}{(U_0 - c)^2} - k^2 \right] w = 0, \quad (7)$$

where

$$\left. \begin{aligned} U_0 &= +U, & \text{for } z > 0 & \text{ [known as region ①]} \\ U_0 &= -U, & \text{for } z < 0 & \text{ [known as region ②]} \end{aligned} \right\}$$

In addition,

$$u = -\frac{i}{k} \frac{dw}{dz}, \quad (8)$$

$$\frac{\rho}{\rho_0} = \frac{N^2/g}{ik(U_0 - c)} w, \quad (9)$$

$$\Phi = \frac{p}{\rho_0} = \frac{U_0 - c}{ik} \frac{dw}{dz}. \quad (10)$$

If  $Z$  is the vertical displacement associated with a particular disturbance, then

$$w = ik(U_0 - c)Z. \quad (11)$$

In general,  $c = c_r + ic_i$ . We shall assume  $c_r = 0$ . At  $z = 0$  we require continuity of  $\Phi$  and  $w/(U_0 - c)$  (*viz.* Drazin and Howard, 1966). As  $z \rightarrow \pm \infty$ , it is required that solutions be bounded. However, for wave solutions, where boundedness does not uniquely determine the solution, the radiation condition is invoked.

### 3. Neutral solutions: $c_i = 0$

I shall first examine neutral solutions for which  $c_i = 0$ . Eq. (7) is now the same in regions ① and ②. The

nature of the solutions depends on whether  $N^2/(k^2U^2)$  is greater than or less than 1.

#### a. $N^2/(k^2U^2) > 1$

Since  $kU$  is the wave frequency observed moving with the mean flow,  $N^2/(k^2U^2) > 1$  is simply a statement that the wave frequency is less than the Brunt-Väisälä frequency. The relevant solutions to (7) and (10) are

$$w = Ae^{inz}, \quad (12)$$

$$\Phi = -\frac{n}{k} U_0 w, \quad (13)$$

$$n = \pm \left( \frac{N^2}{U^2} - k^2 \right)^{\frac{1}{2}}. \quad (14)$$

For the above solutions it is necessary to impose the radiation condition at  $z \rightarrow \pm \infty$ ; i.e.,

$$\overline{\Phi w} > 0, \quad \text{for } z > 0, \quad (15)$$

$$\overline{\Phi w} < 0, \quad \text{for } z < 0, \quad (16)$$

where the overbar refers to an average over a single wavelength in the  $x$  direction. From (12) and (13) we see that this implies  $n > 0$  in both regions ① and ②, so that

$$w_1 = A_1 e^{inz}, \quad (17)$$

$$w_2 = A_2 e^{inz}. \quad (18)$$

Continuity of  $\Phi$  at  $z = 0$  implies

$$A_1 = -A_2. \quad (19)$$

When (19) is satisfied, it is easily shown that for solutions (17) and (18),  $w/U_0$  is continuous at  $z = 0$  as well. Thus for all  $k^2$  in  $(0, N^2/U^2)$ , there exist neutral internal-gravity wave solutions satisfying radiation conditions at both  $z = +\infty$  and  $z = -\infty$ .

#### b. $N^2/(k^2U^2) < 1$

For this case the solutions in regions ① and ② are

$$w_1 = A_1 e^{-n_1 z}, \quad (20)$$

$$w_2 = A_2 e^{n_2 z}, \quad (21)$$

$$\Phi_1 = -\frac{nA_1}{ik} U e^{-n_1 z}, \quad (22)$$

$$\Phi_2 = -\frac{nA_2}{ik} U e^{n_2 z}, \quad (23)$$

$$n = + \left( k^2 - \frac{N^2}{U^2} \right)^{\frac{1}{2}}. \quad (24)$$

Continuity of  $\Phi$  at  $z=0$  requires

$$A_1 = A_2. \tag{25}$$

When (25) is satisfied it can be shown that it is impossible for  $w/U_0$  to be continuous at  $z=0$  (except in the trivial case where  $A_1=0$ ). Thus, there exist no neutral solutions for  $k^2 > N^2/U^2$ .

**4. Unstable solutions:  $c_i \neq 0$**

In this case, we have complex values for  $n$  [as used in Eqs. (20) and (21), for example] given by

$$n_1^2 = k^2 - \frac{N^2}{(U - ic_i)^2}, \tag{26}$$

$$n_2^2 = k^2 - \frac{N^2}{(U + ic_i)^2} = n_1^{2*}, \tag{27}$$

where the asterisk refers to the complex conjugate. Since the  $n_2$ 's are the complex conjugates of the  $n_1$ 's, we may choose  $n_1$  to be that solution of (26) with a positive real part, and, invoking boundedness, the relevant solutions may be written:

$$w_1 = A_1 e^{-n_1 z}, \tag{28}$$

$$w_2 = A_2 e^{n_1^* z}, \tag{29}$$

$$ik\Phi_1 = (U - ic_i)(-n_1)A_1 e^{-n_1 z}, \tag{30}$$

$$ik\Phi_2 = (-U - ic_i)(n_1^*)A_2 e^{n_1^* z}. \tag{31}$$

Note that in the event  $\text{Re}(n_1)=0$ , Eqs. (28)–(31) satisfy the radiation conditions as described in Section 3a.

The continuity of  $\Phi$  at  $z=0$  implies

$$-(U - ic_i)n_1 A_1 = -(U + ic_i)n_1^* A_2, \tag{32}$$

while the continuity of  $w/(U_0 - c)$  implies

$$-(U + ic_i)A_1 = (U - ic_i)A_2. \tag{33}$$

The consistency of (32) and (33) imply

$$(U - ic_i)^2 n_1 = -(U + ic_i)^2 n_1^*. \tag{34}$$

Since the right-hand side of (34) is minus the complex conjugate of the left-hand side,

$$\text{Re}[(U - ic_i)^2 n_1] = 0, \tag{35}$$

or

$$n_{1r} = -\frac{2c_i U}{(U^2 - c_i^2)} n_{1i}, \tag{36}$$

where

$$n_1 = n_{1r} + in_{1i}.$$

Eqs. (26) and (36) may be shown to be consistent in two cases:

$$(i) \quad c_i = 0, \quad n_{1r} = 0, \quad n_{1i}^2 = \frac{N^2}{U^2} - k^2, \quad k^2 < \frac{N^2}{U^2}.$$

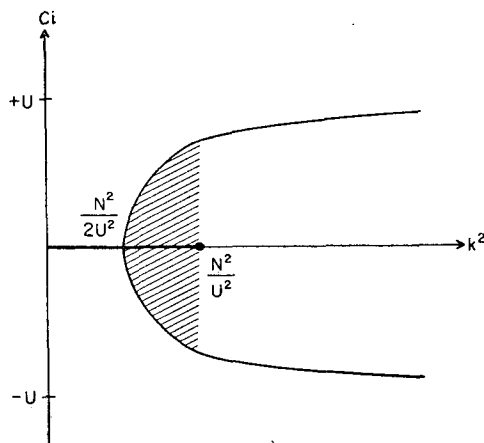


FIG. 2. Stability curve:  $c_i$  vs  $k^2$ .

This case is exactly that investigated in Section 3.

(ii)  $c_i \neq 0$ .

In this case

$$c_i^2 = U^2 - \frac{N^2}{2k^2}, \tag{37}$$

and

$$k^2 > N^2/(2U^2),$$

$$n^2 = -\frac{k^2(U + ic_i)^2}{(U - ic_i)^2}. \tag{38}$$

Eq. (38) implies  $|n|^2 = k^2$ .

The above results are readily compared with the results for the Helmholtz problem (the above problem with  $N^2=0$ ) where  $c_i^2 = U^2$  for all  $k^2$  and  $n^2 = k^2$ . The fact that  $N^2 \neq 0$  eliminates instability for  $k^2 < N^2/(2U^2)$ .

Combining the results of this section and those of Section 3 leads to the stability diagram shown in Fig. 2. Because of stratification, we have neutral wave solutions for  $k^2 < N^2/U^2$ ; also because of stratification, instability is suppressed for  $k^2 < N^2/(2U^2)$ . For  $N^2/(2U^2) < k^2 < N^2/U^2$  neutral, stable and unstable solutions may all exist. As mentioned in the Introduction the coexistence of neutral internal waves (which, in principle, may propagate indefinitely far from the shear zone) and instabilities (which are exponentially confined to the shear zone) is qualitatively consistent with observed aspects of clear air turbulence. Quantitative comparisons will be made in Section 7.

It should be reemphasized that both the neutral waves and the instabilities can act to smooth the shear zone—the former by propagating energy and momentum away from the shear zone, the latter by growing at the expense of the energy in the mean flow. It will be the purpose of Sections 5–7 to estimate the relative importance of these processes.

### 5. Modification of the basic flow

As already noted, both neutral propagating waves and instabilities can serve to smooth out the original Helmholtz flow profile. It will be assumed, in this section, that such smoothing occurs until

$$\text{Ri} = N^2 \int \left( \frac{dU_0}{dz} \right)^2 \approx \frac{1}{4}. \quad (39)^1$$

For  $\text{Ri} > \frac{1}{4}$  no instabilities exist (Howard, 1961). Also, implicit in the work of Booker and Bretherton (1967) and Jones (1968) is the fact that neutral wave solutions also do not exist when  $\text{Ri} > \frac{1}{4}$ . A heuristic demonstration of the latter effect is offered in Appendix A.

I now wish to estimate under what conditions propagation or instability will dominate the smoothing. For a crude first estimate I will adopt the following procedure:

- (i) Calculate the reduction in kinetic energy between the Helmholtz profile and one for which  $\text{Ri} = \frac{1}{4}$ . This difference will be called  $\Delta E$ .
- (ii) Using the solutions for an unsmoothed Helmholtz profile, estimate the time for propagating waves to carry away  $\Delta E$  (this time will be called  $\tau_w$ ).
- (iii) Using the solutions for an unsmoothed Helmholtz profile, estimate the time for unstable waves to increase in energy by  $\Delta E$  (this time will be called  $\tau_i$ ).

Clearly both  $\tau_w$  and  $\tau_i$  will depend on the magnitude of the initial perturbation. Also, since the probable diminution of the fluid's ability to sustain both neutral waves and instabilities as the original shear is smoothed has been neglected, the values obtained for  $\tau_i$  and  $\tau_w$  are probably substantial underestimates. It is nevertheless hoped that the relative sizes of  $\tau_i$  and  $\tau_w$  will be indicative of which is more important in eliminating the original instability. In particular, if  $\tau_w < \tau_i$  propagation should be more important, and for  $\tau_i < \tau_w$  the reverse should be true.

#### a. The kinetic energy difference $\Delta E$

In Fig. 1 are shown both the original Helmholtz profile and a profile where the original velocity discontinuity has been smoothed over a distance  $2d$  in order that  $\text{Ri} = \frac{1}{4}$ , where

$$\text{Ri} = \frac{N^2}{(U/d)^2}.$$

The value  $\text{Ri} = \frac{1}{4}$  implies

$$d = U/(2N). \quad (40)$$

<sup>1</sup>This is only an assumption. It is certainly conceivable that conditions may exist, for example, where an unstable perturbation will grow until some steady finite amplitude is reached with the mean flow remaining somewhat unstable. However, I shall not concern myself with such situations here.

The difference in kinetic energy between the two profiles is entirely due to the region  $-d < z < d$ :

$$\frac{1}{2} \text{KE}_{\text{Helmholtz}} = \frac{1}{2} \rho_0 \int_0^d U^2 dz = \frac{\rho_0}{2} d U^2 = \frac{1}{2} \rho_0 \frac{U^3}{2N}, \quad (41)$$

$$\frac{1}{2} \text{KE}_{\text{neutral}} = \frac{1}{2} \rho_0 \int_0^d \frac{U^2 z^2}{d^2} dz = \frac{\rho_0}{2} \frac{d U^2}{2} = \frac{1}{2} \rho_0 \frac{U^3}{6N}, \quad (42)$$

$$\frac{1}{2} \Delta E = \frac{\rho_0}{6} \frac{U^3}{N}. \quad (43)$$

#### b. The time $\tau_w$

The vertical energy flux is given by

$$\overline{pw} = \rho_0 \frac{n}{k} U \frac{1}{2} |w|^2, \quad (44)$$

where  $|w|$  is the amplitude of  $w$ , and the factor  $\frac{1}{2}$  arises from averaging over a cycle. In general, it is more meaningful to specify perturbations in terms of  $Z$  rather than  $w$  [see (11)]; we also use (14) to replace  $n$  in (44). The result is

$$\overline{pw} = \rho_0 \frac{\left( \frac{N^2}{U^2} - k^2 \right)^{\frac{1}{2}}}{k} U \frac{1}{2} k^2 U^2 |Z_k|^2, \quad (45)$$

where  $Z_k$  is the height perturbation associated with wavenumber  $k$ . From (45) we see that for a given magnitude of  $Z$ , there exists a  $k$  which maximizes  $\overline{pw}$ ; this  $k$  will be called  $k_{\text{opt}}$  which can be shown to be

$$k_{\text{opt}}^2 = \frac{N^2}{2U^2}. \quad (46)$$

For  $k_{\text{opt}}$  (46) becomes

$$\overline{pw}_{\text{opt}} = \frac{1}{4} \rho_0 U N^2 |Z_{k_{\text{opt}}}|^2. \quad (47)$$

Note that  $\overline{pw}$  is only half the energy loss since waves are propagating both upward above  $z=0$  and downward below  $z=0$ . Thus

$$\tau_w = \frac{1}{2} \Delta E / \overline{pw}_{\text{opt}},$$

and using (43) and (47)

$$\tau_w = \frac{2}{3} \frac{U^2}{N^3 |Z_{\text{opt}}|^2}. \quad (48)$$

#### c. The time $\tau_i$

It is readily shown that the energy density for a perturbation in our Boussinesq fluid is

$$E = \frac{1}{2} \rho_0 \left[ u^2 + w^2 + \frac{g^2}{N^2} \left( \frac{\rho}{\rho_0} \right)^2 \right]. \quad (49)$$

We now wish to evaluate

$$\int_0^\infty \bar{E} dz.$$

It is shown in Appendix B that for the unstable perturbations of Section 4,

$$\int_0^\infty \bar{E} dz = \frac{1}{8n_r} e^{2k c_i t} |w_0(k)|^2 \left[ 2 + \frac{N^2}{k^2(U^2 + c_i^2)} \right] \rho_0, \quad (50)$$

where  $n_r$  is the real part of  $n$ , and  $|w_0(k)|$  the amplitude of the  $w$  perturbation at  $t=0$  and  $z=0$ .

The question now arises as to what value of  $k$  (and hence  $n_r$  and  $c_i$ ) to choose. While the disturbance growth rate increases as  $k$  increases, the larger  $k$ 's are associated with  $n$ 's [recall from (38) that  $|n| = |k|$ ] whose vertical scales are short compared with  $d = U/(2N)$  and which cannot be expected to smooth out shears over a scale  $d$ . I will therefore select that  $k$  for which  $n_r = 2N/U$ .

It may be shown from (37) and (38) that

$$\frac{n_r}{k} = \left( 1 - \frac{N^2}{2k^2 U^2} \right)^{\frac{1}{2}} / \left( 1 - \frac{N^2}{4k^2 U^2} \right). \quad (51)$$

Setting  $n_r = 2N/U$  in (51) yields

$$\frac{2N}{kU} = \left( 1 - \frac{N^2}{2k^2 U^2} \right)^{\frac{1}{2}} / \left( 1 - \frac{N^2}{4k^2 U^2} \right). \quad (52)$$

We let  $\mu = N/(Uk)$  and let  $\mu_c$  be that value of  $\mu$  which satisfies (52); i.e.,

$$2\mu_c = (1 - \frac{1}{2}\mu_c^2)^{\frac{1}{2}} / (1 - \frac{1}{4}\mu_c^2). \quad (53)$$

Eq. (53) may be approximately solved. One finds

$$\mu_c \approx 0.5, \quad (54)$$

from which one then finds

$$k_c \approx 2 \frac{N}{U}, \quad (55)$$

$$c_i^2 = U^2 (1 - \frac{1}{2}\mu_c^2) \approx 0.875 U^2, \quad (56)$$

$$c_i \approx 0.935 U.$$

Using the above, and again replacing  $|w_0|$  with  $kU|Z_0|$ , (50) becomes

$$\int_0^\infty \bar{E} dz \approx 0.533 \rho_0 U N |Z_0|^2 e^{3.74 N t}. \quad (57)$$

Eq. (57) represents half the perturbation energy (only the region  $z \geq 0$  has been considered). We want the difference in

$$\int_0^\infty \bar{E} dz$$

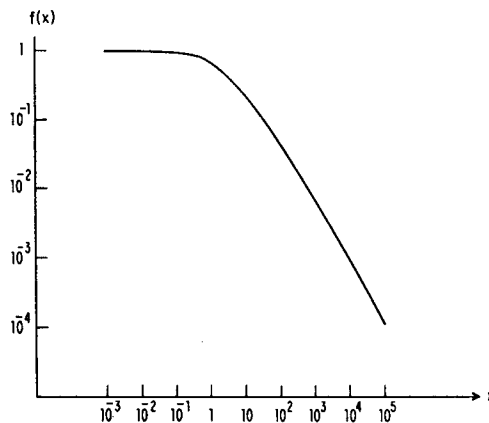


FIG. 3.  $f(x) = x^{-1} \log(1+x)$  as a function of  $x$ .

between  $t=0$  and  $t = \tau_i$  to equal  $\frac{1}{2} \Delta E$ ; i.e.,

$$0.533 U N |Z_{2N/U}|^2 \rho_0 (e^{3.74 N \tau_i} - 1) \approx \frac{\rho_0 U^3}{6 N}, \quad (58)$$

or

$$\tau_i \approx \frac{1}{3.74 N} \ln \left( 1 + 0.3125 \frac{U^2}{N^2 |Z_{2N/U}|^2} \right). \quad (59)$$

#### d. Comparison of $\tau_i$ and $\tau_w$

Using (48) and (59) one finds

$$\frac{\tau_i}{\tau_w} \approx 0.1253 \frac{|Z_{N/(\sqrt{2}U)}|^2 \ln(1+x)}{|Z_{2N/U}|^2 x}, \quad (60)$$

where

$$x \approx 0.3125 \frac{U^2}{N^2 |Z_{2N/U}|^2}.$$

The function  $f(x) = x^{-1} \ln(1+x)$ , a positive monotonically decreasing function of  $x$ , where  $f(0) = 1$ , is plotted in Fig. 3. Thus for  $\tau_i/\tau_w \approx 1$

$$|Z_{N/\sqrt{2}U}| > 2.825 |Z_{2N/U}|. \quad (61)$$

In general,  $x \gg 1$  and  $f(x) \ll 1$  so that  $|Z_{N/\sqrt{2}U}|/|Z_{2N/U}|$  must be even greater than indicated in (61) for  $\tau_i/\tau_w \approx 1$ . On the other hand, it may be that in the unstable  $k$  region, half of  $Z$  may go into stable decaying modes so that  $|Z_{2N/U}|$  should be divided by 2.

### 6. Clear air turbulence

There is a danger in reading Section 5, that one may confuse effectiveness in smoothing the originally unstable flow field with prominence in the structure of clear air turbulence. Certainly the two are related. However, the fact remains that disturbances with very large wavenumbers  $k$  are most unstable. Even though they are unlikely to contribute to the smoothing of the basic flow over substantial depths, they should be

ubiquitously present at interfaces displaced by the larger scale disturbances. This appears consistent with observations which show the existence of small-scale disturbances within larger scale structures (Reed and Hardy, 1972). Similarly, the results in Section 5 suggest that for given initial height perturbations instability will more efficiently dissipate a shear zone. This, however, does not preclude the possibility that over much of the life of a shear zone, propagating waves will dominate the disturbance field. As will be seen in Section 7 this does seem to be the case in various observed situations. Finally, there is an implication in Section 5 that instabilities of a scale sufficient to smooth the shear profiles over a large enough depth will set on despite the vastly greater instability of shorter scale disturbances. The results of Section 7 lead one to suspect that this is not so.

Thus far, I have avoided discussing Kelvin-Helmholtz instability. This may seem surprising insofar as it has become virtually gospel over the last six years that Kelvin-Helmholtz instability is responsible for clear air turbulence. Indeed this may prove to be the case. Nonetheless, as pointed out in the Introduction virtually all calculations of Kelvin-Helmholtz instability have involved configurations where both shear and stratification disappear outside a thin layer. Thus, the possibility of suppressing instability by permitting energy to be propagated away in the form of internal waves is absent. However, observations generally show that stratification does not disappear outside the shear zone. This has led me to seek how far one might get toward a description of clear air turbulence with the present alternative configuration.

## 7. Specific cases

I shall briefly attempt to discuss in terms of the preceding considerations four cases, where interfacial waves were observed on an unstable shear zone. The cases are taken from published papers and tend to deal with markedly different situations. Some salient features of these cases are summarized in Table 1 which gives the height of the unstable layer, the speed discontinuity  $U$ , the Brunt-Väisälä frequency  $N$ , the wavelength of the interfacial wave, the amplitude  $Z$  of the disturbance height field (one-half the trough-crest distance) and the lifetime of the disturbances (where given). Also shown are the wavelengths for optimal wave flux generation [ $2\pi\sqrt{2}U/N$ ] and for the shortest instability with sufficient vertical scale to stabilize the Helmholtz profile [ $2\pi U/(2N)$ ].

In every case the primary observed wavelength is approximately the wavelength for optimal wave flux generation, although in case 4 relatively short wavelengths were observed as well. In a study not summarized in Table 1, Metcalf and Atlas (1973) indeed found virtually all resolvable wavelengths. It should be pointed out that the main observed wavelengths are

also what one would expect from Kelvin-Helmholtz instability where  $N$  is taken to be the Brunt-Väisälä frequency in the shear zone<sup>2</sup>.

However, the values of  $N$  in Table 1 are characteristic of a broader region. In cases where the Kelvin-Helmholtz mechanism is plausible one would expect larger values of  $N$  in the shear zone and hence shorter wavelengths.

If we interpret the observed disturbances as internal gravity waves being fed by the unstable shear zone, we are led to some additional problems. In Table 2 I show for each of the cases in Table 1, the value of  $\tau_w$  [given by Eq. (48) identifying  $Z$  with  $Z_w$ ] and that value of  $Z_i$  (at  $t=0$ ) which would make  $\tau_i \approx \tau_w$ . We see that  $\tau_w$  appears to be substantially shorter than observed lifetimes and that only very small initial perturbations at unstable wavelengths would be necessary to stabilize the profile with comparable rapidity. In the context of the present crude and uncertain calculations we are led to the following tentative conclusions:

- (i) Those forces tending to create the unstable shear zone are continuing to act during the observed lifetime of the disturbances.
- (ii) Instabilities of a scale sufficient to stabilize the shear zone are somewhat suppressed *relative* to the internal waves, or, conversely, the waves are selectively enhanced.
- (iii) Instabilities of very short scales are indeed observed.

## 8. Some additional remarks

If the disturbances described in Section 7 are internal gravity waves, then their vertical wavelengths will be about the same as their horizontal wavelengths [*viz.* Eqs. (14) and (46)], and in at least cases 2, 3 and 4 this wavelength is larger than the distance between the shear layer and the ground. Thus, the assumption in Section 3 that boundaries are infinitely far away is unlikely to be correct, at least as concerns the limit  $z \rightarrow -\infty$ . Instead, it is to be expected that a wave emitted downward will be reflected at the ground and returned to the shear zone. Our present calculations are unable to predict what will happen at this stage. However, the problem has, in many ways, been anticipated by Jones (1968) who considered the reflection of internal gravity waves at a critical level (where their Doppler-shifted frequency was zero). He found that when the Richardson number at the critical level was less than 0.25, over-reflection occurred; i.e., the amplitude of the reflected wave exceeded that of the incoming wave. In fact, the results of Section 3a may be

<sup>2</sup> Miles and Howard (1964) show that the most unstable Kelvin-Helmholtz wave has a wavelength which is  $\sim 7.5(2d)$ . Assuming  $Ri \approx \frac{1}{2}$  and  $d \approx U/(2N)$ , the wavelength is  $7.5 U/N$  as opposed to  $2\pi\sqrt{2}U/N \approx 8.89U/N$ .

TABLE 1. Observed disturbances in shear zones and theoretical values for two wavelengths.\*

	ht (km)	<i>U</i> (m sec <sup>-1</sup> )	<i>N</i> (sec <sup>-1</sup> )	Observed wavelength	Observed <i>Z</i>	Lifetime	$\frac{2\pi\sqrt{2}U}{N}$	$\frac{2\pi U}{2N}$
Case 1 Wallops Is., Va. 7 February 1968 (Ottersten <i>et al.</i> , 1973)	11	10	$2 \times 10^{-2}$	6 km	250 km	not reported	4.44 km	1.57 km
Case 2 Haswell, Colo. 12 November 1971 (Hooke <i>et al.</i> , 1973)	0.12	1	$2.7 \times 10^{-2}$	350 m	15 m	10 min	329 m	116 m
Case 3 Wallops Is., Va. 19 February 1970 (Hardy <i>et al.</i> , 1973)	2.5	7	$2 \times 10^{-2}$	2.7 km	250 m	10 min	3.1 km	1.1 km
Case 4 Wallops Is., Va. (Reed and Hardy, 1972)	9	28	$1.3 \times 10^{-2}$	15-20 km†	1 km	not reported	19.1 km	6.8 km

\* See text for definitions.

† 1.6 km wavelength billows also observed.

considered an extreme case of Jones' results; i.e., infinite over-reflection where there are outgoing waves from the critical level without any incoming waves. In any case, with over-reflection we may conjecture that the return of the wave reflected by the ground will lead to increased radiation of the internal wave by the shear zone, and perhaps to an explosive instability. This may be the reason that the wave solutions appear to dominate the conventionally unstable modes in the observed cases.

It should be added that the solution described in Section 3a is consistent with the initially braided structure of observed disturbances. In particular, the perturbation velocities on opposite sides of the shear interface are oppositely directed [*viz.* Eqs. (17)-(19)]. Whether, under the influence of a broadening shear zone and the return of waves reflected from the ground, a cat's eye structure would develop, remains an open question.

9. Conclusions

The discussion of Section 8 suggests a number of calculations which would serve to make the present work more relevant to observed disturbances in atmospheric shear zones. However, at this point, I hope I have at least shown that unstable shear zones can radiate internal gravity waves, and that these waves

can supplement and perhaps supplant Kelvin-Helmholtz instability in explaining clear air turbulence.

*Acknowledgment.* This work has been supported by Grant GA 33990X from the National Science Foundation.

APPENDIX A

Nonexistence of Neutral Waves for  $Ri > \frac{1}{4}$

In Booker and Bretherton (1967) it is shown that for  $Ri > \frac{1}{4}$ , the continuation of an upward wave energy flux  $F_1$  for  $z > 0$  is an upward wave flux

$$F_1 \exp[2\pi(Ri - \frac{1}{4})z], \text{ for } z < 0.$$

Similarly, the continuation of a downward wave flux  $F_2$  for  $z < 0$  is a downward flux

$$F_2 \exp[2\pi(Ri - \frac{1}{4})z], \text{ for } z > 0.$$

Thus, for  $Ri > \frac{1}{4}$  it is impossible to have fluxes purely outward from  $z = 0$ .

APPENDIX B

Total Energy

Our fields are generally written in the complex form for unstable solutions

$$f = \int e^{ikx} e^{kct} e^{-nz},$$

where  $f$  and  $n$  are complex constants. For Eqs. (49) and (50), however, we wish the real parts of such expressions. In particular we wish to evaluate integrals of the form

$$\int_0^\infty \overline{(Re f)}^2 dz.$$

TABLE 2.

Case	$\tau_w$ (sec)	$Z_i$ (m)
1	133	1.9
2	150	0.01
3	65	17
4	237	3.73

Now,

$$\begin{aligned} \text{Ref} &= (f_r \cos kx - f_i \sin kx) e^{-nrz} e^{kci t} \cos n_i z \\ &\quad + (f_r \sin kx + f_i \cos kx) e^{-nrz} e^{kci t} \sin n_i z, \\ (\text{Ref})^2 &= e^{-2nrz} e^{2kci t} [(f_r^2 \cos^2 kx - 2f_r f_i \cos kx \sin kx \\ &\quad + f_i^2 \sin^2 kx) \cos^2 n_i z + 2(f_r^2 \cos kx \sin kx + f_r f_i \cos^2 kx \\ &\quad - f_r f_i \sin^2 kx - f_i^2 \sin kx \cos kx) \cos n_i z \sin n_i z \\ &\quad + (f_r^2 \sin^2 kx + 2f_r f_i \sin kx \cos kx + f_i^2 \cos^2 kx) \sin^2 n_i z], \\ (\text{Ref})^2 &= e^{-2nrz} e^{2kci t} \left[ \frac{1}{2} (f_r^2 + f_i^2) \cos^2 n_i z \right. \\ &\quad \left. + \frac{1}{2} (f_r^2 + f_i^2) \sin^2 n_i z \right] \\ &= e^{-2nrz} e^{2kci t} \left[ \frac{1}{2} (f_r^2 + f_i^2) \right] \\ &= \frac{1}{2} \hat{f} \hat{f}^* e^{-2nrz} e^{2kci t}. \end{aligned}$$

Thus

$$\int_0^\infty \overline{(\text{Ref})^2} dz = \frac{1}{2} \hat{f} \hat{f}^* e^{2kci t} \frac{1}{2n_r}, \quad (\text{B1})$$

where

$$\left. \begin{aligned} \hat{f} &= f_r + i f_i \\ n &= n_r + i n_i \end{aligned} \right\}$$

Using (B1) it is readily shown that

$$\left. \begin{aligned} \int_0^\infty \overline{(\text{Rew})^2} dz &= \frac{1}{4n_r} |w_0|^2 e^{2kci t} \\ \int_0^\infty \overline{(\text{Reu})^2} dz &= \frac{1}{4n_r} \frac{|n_1|^2}{k^2} |w_0|^2 e^{2kci t} \\ \int_0^\infty \overline{\left( \frac{\rho}{\rho_0} \right)^2} dz &= \frac{1}{4n_r} \frac{(N^2/g)^2}{k^2(U^2 + c_i^2)} |w_0|^2 e^{2kci t} \end{aligned} \right\} \quad (\text{B2})$$

which when inserted in (49) yield

$$\int_0^\infty \bar{E} dz = \frac{\rho_0}{8n_r} e^{2kci t} |w_0|^2 \left[ \frac{|n_1|^2}{k^2} + 1 + \frac{g^2}{N^2} \frac{(N^2/g)^2}{k^2(U^2 + c_i^2)} \right]. \quad (\text{B3})$$

Using  $|n_1|^2 = k^2$  we finally obtain Eq. (50).

#### REFERENCES

- Booker, J. R., and F. B. Bretherton, 1967: The critical layer for internal gravity waves in a shear flow. *J. Fluid Mech.* **27**, 513-539.
- Drazin, P. G., and L. N. Howard, 1966: Hydrodynamic stability of parallel flow of inviscid fluids. *Advances in Applied mechanics*, Vol. 9, New York, Academic Press, 1-89.
- Hardy, K. R., R. J. Reed and G. K. Mather, 1973: Observation of Kelvin-Helmholtz billows and their mesoscale environment by radar, instrumental aircraft, and a dense radiosonde network. *Quart. J. Roy. Meteor. Soc.* **99**, 279-293.
- Hines, C. O. 1960: Internal gravity waves at ionospheric heights. *Can. J. Phys.*, **38**, 1441-1481.
- Hooke, W. H., F. F. Hall, Jr., and E. E. Gossard, 1973: Observed generation of an atmospheric gravity wave by shear instability in the mean flow of the planetary boundary layer. *Boundary-Layer Meteor.*, **5**, 29-42.
- Howard, L. N., 1961: Note on a paper of John W. Miles. *J. Fluid Mech.*, **10**, 509-512.
- Jones, W. L., 1968: Reflexion and stability of waves in stably stratified fluids with shear flow: A numerical study. *J. Fluid Mech.*, **34**, 609-647.
- Metcalfe, J. I., and D. Atlas, 1973: Microscale ordered motions and atmospheric structure associated with thin echo layers in stably stratified zones. *Boundary-Layer Meteor.*, **4**, 7-36.
- Miles, J. W., and L. N. Howard, 1964: Note on a heterogeneous shear flow. *J. Fluid Mech.*, **20**, 331-336.
- Ottensten, H., K. R. Hardy and C. G. Little, 1973: Radar and sodar probing of waves and turbulence in statically stable clear-air layers. *Boundary-Layer Meteor.*, **4**, 47-90.
- Reed, R. J., and K. R. Hardy, 1972: A case study of persistent, intense clear air turbulence in an upper level frontal zone. *J. Appl. Meteor.*, **11**, 541-549.